Diverse molecular causes of unsolved autosomal dominant tubulointerstitial kidney diseases

Wopperer, Florian J.; Knaup, Karl X.; Stanzick, Kira J.; Schneider, Karen; Jobst-Schwan, Tilman; Ekici, Arif B.; Uebe, Steffen; Wenzel, Andrea; Schliep, Stefan; Schürfeld, Carsten; ...

Diverse molecular causes of unsolved autosomal dominant tubulointerstitial kidney diseases

OPEN

Florian J. Wopperer[1,2], Karl X. Knaup[1], Kira J. Stanzick[3], Karen Schneider[1], Tilman Jobst-Schwan[1,2], Arif B. Ekici[4], Steffen Uebe[4], Andrea Wenzel[5], Stefan Schliep[6], Carsten Schürfeld[7], Randolf Seitz[8], Wanja Bernhardt[9], Markus Gödel[10], Antje Wiesener[4], Bernt Popp[4,11], Klaus J. Stark[3], Hermann-Josef Gröne[12,13], Björn Friedrich[14], Martin Weiß[15], Nikolina Basic-Jukic[16], Mario Schiffer[1], Bernd Schröppel[17], Bruno Huettel[18], Bodo B. Beck[5], Genomics England Research Consortium, John A. Sayer[19], Christine Ziegler[20], Maike Büttner-Herold[21], Kerstin Amann[21], Iris M. Heid[3], André Reis[4], Francesca Pasutto[4,22] and Michael S. Wiesener[1,22]

[1]Department of Nephrology and Hypertension, University Hospital Erlangen, Friedrich-Alexander University Erlangen-Nürnberg, Erlangen, Germany; [2]Research Center on Rare Kidney Diseases (RECORD), University Hospital Erlangen, Erlangen, Germany; [3]Department of Genetic Epidemiology, University of Regensburg, Regensburg, Germany; [4]Institute of Human Genetics, University Hospital Erlangen, Friedrich-Alexander University Erlangen-Nürnberg, Erlangen, Germany; [5]Institute of Human Genetics, Center for Molecular Medicine Cologne (CMMC), and Center for Rare Disease (ZSEK), University Hospital of Cologne, Cologne, Germany; [6]Department of Dermatology, University Hospital Erlangen, Friedrich-Alexander University Erlangen-Nürnberg, Erlangen, Germany; [7]Gesundheitszentrum Vauban, Saarlouis, Germany; [8]Department of Nephrology and Hypertension, Klinikum Neumarkt, Neumarkt, Germany; [9]Zentrum für Nieren-, Hochdruck- und Stoffwechselerkrankungen, Hannover, Germany; [10]III. Department of Medicine, University Medical Center Hamburg-Eppendorf, Hamburg, Germany; [11]Institute of Human Genetics, University of Leipzig Hospitals and Clinics, Leipzig, Germany; [12]Medical Faculty, University of Heidelberg, Heidelberg, Germany; [13]Institute of Pharmacology, University of Marburg, Marburg, Germany; [14]Nephrologisches Zentrum Böblingen Leonberg Herrenberg, Leonberg, Germany; [15]Walddörfer-Dialyse, Hamburg, Germany; [16]Department of Nephrology, Arterial Hypertension, Dialysis and Transplantation, University Hospital Centre Zagreb, Zagreb, Croatia; [17]Sektion Nephrologie, Klinik für Innere Medizin I, Universität Ulm, Ulm, Germany; [18]The Max Planck-Genome-Centre Cologne, Max Planck Institute for Plant Breeding Research, Cologne, Germany; [19]Translational and Clinical Research Institute, Faculty of Medical Sciences, Newcastle University, Newcastle Upon Tyne, UK; [20]Department of Biophysics, University of Regensburg, Regensburg, Germany; and [21]Department of Nephropathology, Institute of Pathology, University Hospital Erlangen, Friedrich-Alexander University Erlangen-Nürnberg, Erlangen, Germany

Autosomal Dominant Tubulointerstitial Kidney Disease (ADTKD) is caused by mutations in one of at least five genes and leads to kidney failure usually in mid adulthood. Throughout the literature, variable numbers of families have been reported, where no mutation can be found and therefore termed ADTKD-not otherwise specified. Here, we aim to clarify the genetic cause of their diseases in our ADTKD registry. Sequencing for all known ADTKD genes was performed, followed by SNaPshot minisequencing for the dupC (an additional cytosine within a stretch of seven cytosines) mutation of *MUC1*. A virtual panel containing 560 genes reported in the context of kidney disease (nephrome) and exome sequencing were then analyzed sequentially. Variants were validated and tested for segregation. In 29 of the 45 registry families, mutations in known ADTKD genes were found, mostly in *MUC1*. Sixteen families could then be termed ADTKD-not otherwise specified, of which nine showed diagnostic variants in the nephrome (four in *COL4A5*, two in *INF2* and one each in *COL4A4*, *PAX2*, *SALL1* and *PKD2*). In the other seven families, exome sequencing analysis yielded potential disease associated variants in novel candidate genes for ADTKD; evaluated by database analyses and genome-wide association studies. For the great majority of our ADTKD registry we were able to reach a molecular genetic diagnosis. However, a small number of families are indeed affected by diseases classically described as a glomerular entity. Thus, incomplete clinical phenotyping and atypical clinical presentation may have led to the classification of ADTKD. The identified novel candidate genes by exome sequencing will require further functional validation.

Kidney International (2022) **102,** 405–420; https://doi.org/10.1016/j.kint.2022.04.031

KEYWORDS: ADTKD; Alport syndrome; exome; MITKD; MUC1; UMOD

Correspondence: *Michael S. Wiesener, Department of Nephrology and Hypertension, University Hospital Erlangen, Friedrich-Alexander University Erlangen-Nürnberg, Ulmenweg 18, 91054 Erlangen, Germany. E-mail: michael.wiesener@uk-erlangen.de*

[22]FP and MSW contributed equally as senior authors.

Received 10 December 2021; revised 22 March 2022; accepted 8 April 2022; published online 26 May 2022

Hereditary kidney diseases are manifold and diverse, with several hundred monogenic diseases identified to date.[1–3] With significant improvement in molecular diagnostics, the weight of genetics in nephrology has greatly increased over the last years. However, a significant proportion of patients with a genetic cause of their disease will

probably not yet have their (correct) diagnosis. The largest study published to date has yielded diagnostic mutations in almost 10% in unbiased cohorts of patients with chronic kidney disease (CKD).[4] Naturally, the rate of diagnostic findings is considerably increased in populations with a clinical suspicion of hereditary CKD (i.e., positive family history, young age at onset, or syndromic type of disease).[5,6]

Profound difficulties in diagnostics can be encountered with autosomal dominant tubulointerstitial kidney disease (ADTKD). Clinically, this disease is completely unspecific, without characteristic findings in kidney morphology, no or little proteinuria, and bland urinary sediment. Histology merely shows immunonegative tubulointerstitial fibrosis,[7,8] which is not discernible from other diseases, such as hypertensive nephropathy or nephronophthisis. Patients with ADTKD usually reach end-stage renal disease (ESRD) in mid adulthood, which may vary considerably even within families.[9,10] Often, the clearest clinical clue is an autosomal dominant family history, mostly with full penetrance.

Mutations in at least 5 genes can cause ADTKD: *UMOD* (Online Mendelian Inheritance in Man [OMIM] number 603860),[11] *MUC1* (OMIM number 174000),[12] *HNF1B* (OMIM number 137920),[13] *REN* (OMIM number 613092),[14] and *SEC61A1* (OMIM number 617056).[15] According to Kidney Disease: Improving Global Outcomes (KDIGO) recommendations, compatible families with negative genetic testing should be termed ADTKD-NOS ("not otherwise specified").[7] Several studies have analyzed cohorts of ADTKD families, with the percentage of ADTKD-NOS ranging from 23% to 55% (Table 1[10,16–22]). The subtype of ADTKD that is surely the most difficult to detect is caused by *MUC1* mutations, which can currently only be analyzed in few laboratories worldwide, because routine testing will miss the so far known diagnostic variants. To date, only mutations with a single specific frameshift effect of a complex repeat region have been found, where the most frequent mutation is an insertion of an additional cytosine (dupC) within a stretch of 7 cytosines.[12] Interestingly, several other (atypical) mutations have been detected, which all lead to the same frameshift effect (Supplementary Table S1),[18,19,22–24] being highly suggestive that this frameshift protein is specifically pathogenic.[25] Because the detection of these mutations can be extremely challenging, immunodetection of mucin 1 frameshift protein has been established on kidney biopsies[16,22] and urinary smears.[22] However, it is not clear if these cumulative efforts identify all ADTKD-*MUC1* families.

The reason for not yielding a diagnostic mutation in families with suspected ADTKD can be multifaceted. First, the clinically suspected diagnosis may be faulty and another distinct disease overlooked, such as mitochondrial diseases (mitochondrially inherited tubulointerstitial kidney disease [MITKD]).[26] Second, mutations could be too complex to be detected (such as atypical *MUC1* mutations), or mutations in novel candidate genes for ADTKD could be responsible. Therefore, unraveling the molecular causes of ADTKD-NOS is a challenging task and the focus of this study. It required intense work with the respective families and broad application of molecular biology and genetic techniques. These studies are representative for the approach to most hereditary kidney diseases and the developed workflows therefore of general interest in nephrology. Thus, the diagnostic efforts and solutions presented herein go beyond ADTKD and are representative for a timely workup in renal genetics.

METHODS

Patient and ethical approval

All individuals gave written informed consent to all clinical and scientific procedures. The studies were approved by the ethics committee of the Friedrich-Alexander University Erlangen-Nürnberg (approval number: 251_18 B) and fully adhere to the Declaration of Helsinki.

All web resources are listed in the Supplementary Methods in the Supplementary WEB resources list.

DNA isolation and Sanger sequencing

DNA from peripheral blood lymphocytes of patients and their family members was extracted according to standard protocols using FlexiGene Kit (Qiagen).

Complete coding regions of the 5 known ADTKD genes, including flanking intronic/untranslated region sequences, were amplified by polymerase chain reaction (PCR) using appropriate amplification protocols. Primer sequences were selected using Primer3 software (https://primer3.ut.ee/) and were supplied by Thermo Fisher. All primer sequences used are available on request. Purified PCR fragments were sequenced using Big Dye Termination chemistry v.3.1 (Applied Biosystems) on an automated capillary sequencer (Applied Biosystems 3730 Genetic Analyzer) and analyzed using SequencePilot Software (JSI Medical Systems GmbH). GenBank accession numbers NM_000458.3, NM_001204285.1, NM_000537.3, NM_013336.3, and NM_001278614.1 were used as reference sequences for *HNF1B*, *MUC1*, *REN*, *SEC61A1*, and *UMOD*, respectively (http://www.ncbi.nlm.nih.gov/).

SNaPshot minisequencing was additionally performed to detect the dupC mutation of *MUC1*, as previously described.[21]

Single-molecule, real-time sequencing

DNA samples were processed and analyzed as described.[27]

Exome sequencing and copy number variant analysis

Exome sequencing (ES) was performed on an Illumina HiSeq-2500 sequencer (Illumina) using the Twist Human Core Exome with RefSeq add-on panel (Twist Bioscience Inc.) to cover a comprehensive target, >99% of all protein-coding genes. Sequence reads were mapped to the GRCh37 (hg19) reference genome using bwa mem v0.7.17,[28] and the output was written as BAM files through samtools v1.9. Deduplication was performed using picard MarkDuplicates v2.18.21. Targets for local realignment were identified and realigned using Genome Analysis ToolKit (GATK) v3.8RealignerTargetCreator and IndelRealigner, respectively. Reads that are properly mapped to both regular and alternative contigs are assigned a mapping score of 0 by bwa mem v.0.7.17. Using Samtools v1.9 and a custom awk script, the mapping score for these reads was then adjusted to 60 to improve overall coverage. Single-nucleotide variations and small insertions and deletions are called using GATK v3.8, HaplotypeCaller, and UnifiedGenotyper, as well as freebayes v1.2, SNVer Individual, and platypus v0.8.1. Calls from all 5 callers were

Table 1 | Portion of ADTKD-NOS in different cohorts investigated

Publication	Country cohort	Method MUC1 VNTR analysis	NOS in % (NOS of total families investigated)
Knaup *et al.* 2018[16,a]	Germany	Restriction-specific enrichment and detection by SNaPshot minisequencing	40.4 (19 of 47)[b]
Ayasreh *et al.* 2018[17]	Spain	Restriction-specific enrichment and detection by SNaPshot minisequencing	55.3 (31 of 56)
Cormican *et al.* 2019[18]	Ireland	Restriction-specific enrichment and detection by mass spectrometry	37.5 (6 of 16)
Olinger *et al.* 2020[19,c]	United States and Belgium	Restriction-specific enrichment and detection by mass spectrometry	23.2 (135 of 585)[b]
Gong *et al.* 2021[20]	China	Long-range, high-fidelity PCR with NGS	27.8 (5 of 18)

ADTKD, autosomal dominant tubulointerstitial kidney disease; NGS, next-generation sequencing; NOS, not otherwise specified; PCR, polymerase chain reaction; VNTR, variable number of tandem repeats.
[a]Part of this cohort was previously published in Ekici *et al.*[21]
[b]Not reported: *HNF1B*, *REN*, and *SEC61A1*.
[c]Parts of these cohorts were previously published in Bleyer *et al.*[10] and Zivna *et al.*[22]
Only molecular genetic results were considered (no immunodetection).

then consolidated via union and annotated with different annotation databases using Annovar.[29] Variant data were then assessed for rare variants using an in-house analysis tool.[30] A virtual gene panel, herein called *nephrome*, with a total of 560 genes associated with an abnormal renal physiology phenotype, according to the Human Phenotype Ontology database (https://hpo.jax.org/: Human Phenotype Ontology term: HP_0012210, version from March 2020), was first evaluated in all affected family members. If no disease-causing variants were detected, an ES analysis was performed.

As part of the ES analysis, copy number variants were evaluated using the ExomeDepth-Software (version 1.1.15) with all nonrelated exomes of the same run as potential references. Identified candidate copy number variants were confirmed by multiplex ligation-dependent probe amplification using the appropriate SALSA multiplex ligation-dependent probe amplification kits, if available (*SALL1*: P180; *HNF1B*: P241; MRC Holland), according to the manufacturer's instructions.

In silico variant selection and characterization

On the basis of the supposed rare incidence of the phenotype, nonsynonymous and synonymous variants in coding regions, including splice sites, were selected on the basis of a population frequency <1% (the Genome Aggregation Database [gnomAD]): https://gnomad.broadinstitute.org/; dbSNP: https://www.ncbi.nlm.nih.gov/SNP; Clinical significance of Variants (ClinVar): https://www.ncbi.nlm.nih.gov/clinvar/), on a "damaging" computational prediction effect scores using the Sorting Intolerant From Tolerant algorithm (SIFT) (http://sift.jcvi.org), PolyPhen2 (http://genetics.bwh.harvard.edu/pph2/), MutationTaster (http://www.mutationtaster.org/), and MutationAssesor (http://mutationassessor.org), on Combined Annotation Dependent Depletion (CADD) score >15 (http://cadd.gs.washington.edu/home[31]), and on their evolutionary conservation (PhyloP[32], GERP++[33]). In addition, we employed the Exonic Splicing Enhancers Finder (ESEfinder 3.0) algorithm[34] to compare splicing probabilities for wild-type and mutated sequences. For all selected variants, familial segregation with the disease was confirmed. All identified novel candidate genes show expression in human kidney tissues based on University of California, Santa Cruz (https://genome.ucsc.edu), and Human Protein Atlas (https://www.proteinatlas.org/) databases (Supplementary Table S7).

We used the Human Genome Variation Society recommendations[35] for description of sequence variants and the American College of Medical Genetics and Genomics guidelines[36] for variant interpretation.

Sequencing of mitochondrial DNA, analysis of X-inactivation, and database search in the Genomics England 100,000 Genomes project are described in the Supplementary Methods section.

Histologic analysis and immunodetection

Wherever possible, we attempted to collect historical kidney biopsies for pathologic reevaluation. In some cases, the biopsies were not retrievable, but the pathologic report at that time was, which was then taken into consideration.

Collagen IV chain α5 (Col IV[α5]) was stained in skin biopsies, retrieved from the upper arm by punch biopsy (6 mm; kai Europe). The biopsy was divided into equal parts and either fixed in 4% paraformaldehyde (Sigma) or cryoconserved in tissue tec (DiaTec). All sections were cut in 2-µm slides for staining. Commercial antibodies against Col IV(α5) were used at a dilution of 1:50: H52 and H53 (Chondrex Inc.). Detailed staining procedure is provided in the Supplementary Methods section.

Mucin 1 frameshift protein in routine kidney biopsies was stained as described.[16]

Reverse transcriptase–PCR analysis

Details of PCR conditions and primer sequences are provided in the Supplementary Methods.

Association with estimated glomerular filtration rate from genome-wide association study meta-analyses of general population studies

Genes residing genome-wide significant genetic loci associated with quantitative traits derived by genome-wide association study meta-analyses are likely candidates to have a role for the trait under study.[37] We queried the known and newly identified genes related to ADTKD and surrounding regions (gene ± 250 kb) for genetic variants associated with estimated glomerular filtration rate (eGFR).[38] These data from genome-wide association study meta-analyses included >1.2 million individuals, mostly general population-based studies. A gene in a previously identified genetic locus is thus supported by at least one single nuclear polymorphism (SNP) with $P < 5 \times 10^{-8}$ (i.e., genome-wide significant). In addition, genes in regions that contained at least one SNP with an association $P < 1 \times 10^{-4}$ were marked as suggestively associated.

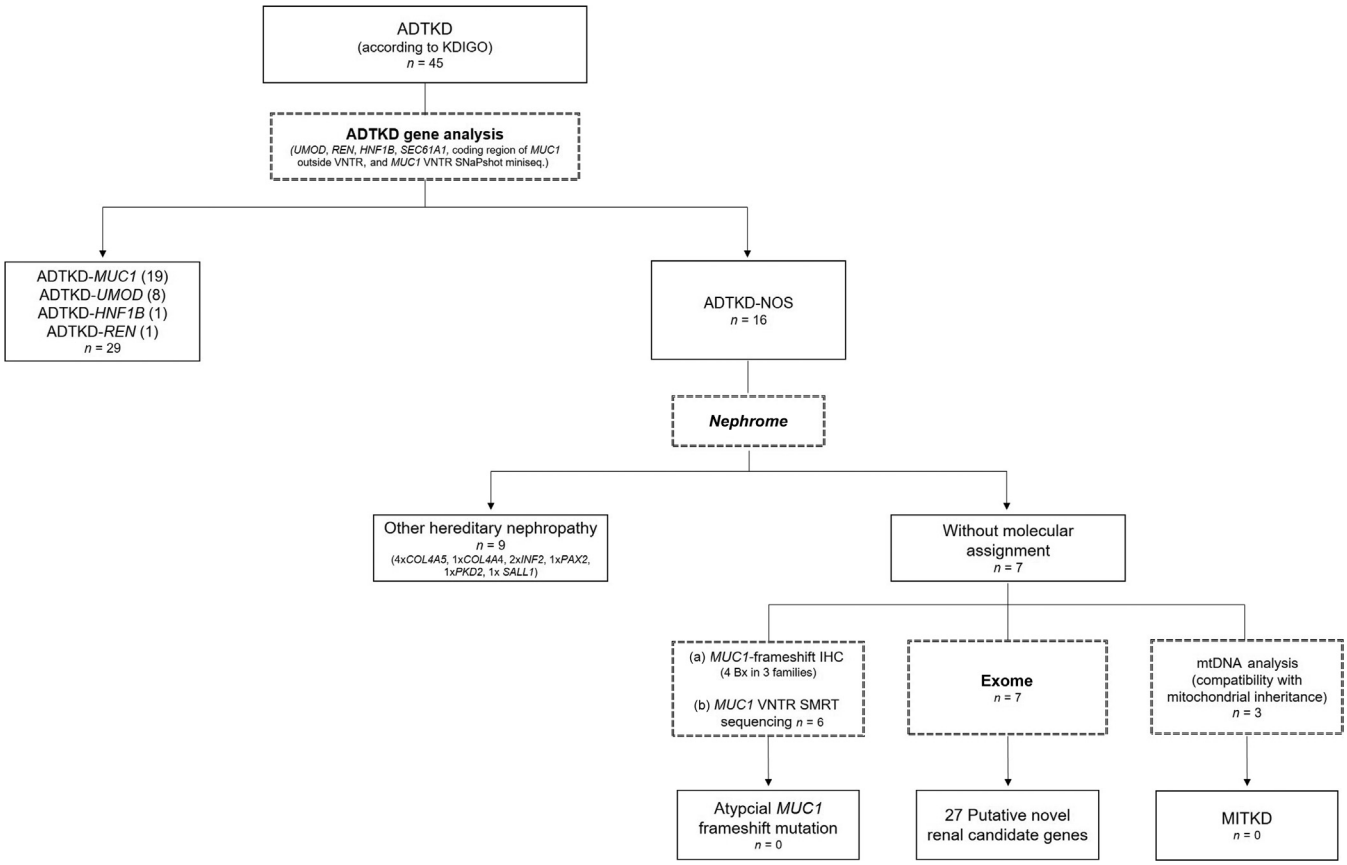

Figure 1 | Flowchart of the diagnostic workflow applied. Index patients of the 45 registry families were primarily sequenced for the known autosomal dominant tubulointerstitial kidney disease (ADTKD) genes (by Sanger sequencing and multiplex ligation-dependent probe amplification analysis until 2017; from 2017 onwards, by next-generation sequencing [NGS]), including SNaPshot minisequencing for the dupC mutation in *MUC1* as well as the coding region of *MUC1* (excluding the VNTR). A total of 29 families showed mutations in known ADTKD genes. No family carried a mutation in *SEC61A1*. The other 16 families were labeled ADTKD-NOS (not otherwise specified) following Kidney Disease: Improving Global Outcomes (KDIGO) guidelines. *Nephrome* analysis, a virtual gene panel consisting of 560 genes associated with abnormal renal physiology, was performed by NGS in the index patients of the respective ADTKD-NOS families, resulting in diagnostic mutations in 9 families. The remaining 7 families were in parallel (*1*) reevaluated for compatibility for mitochondrial disease (i.e., mitochondrial inheritance), (*2*) checked for atypical *MUC1* frameshift mutations by (*a*) immunohistochemistry on kidney biopsies wherever available as well as (*b*) *MUC1* VNTR single-molecule, real-time (SMRT) sequencing, and finally (*3*) exome sequencing by NGS was performed, resulting in 27 putative novel renal candidate genes. Neither atypical *MUC1* frameshift mutations (Supplementary Table S4) nor mitochondrially inherited tubulointerstitial kidney disease (MITKD) has been detected. *n* represents the number of families. Dotted lined boxes indicate the diagnostic tool used. IHC, immunohistochemistry; mtDNA, mitochondrial DNA.

Expression quantitative trait loci variant analyses

Common variants associated with eGFR that also modulate gene expression (expression quantitative trait loci variants [eQTLs]) in kidney tissue can support a gene as relevant for kidney function and can provide additional support for genes with rare SNPs identified for ADTKD. Therefore, we searched for eQTLs in kidney tissue for any of the known and identified candidate genes for ADTKD. We queried 3 types of eQTL data for significant association (false discovery rate, <0.05) on candidate gene expression levels: (i) eQTL in tubulointerstitial tissue from the Nephrotic Syndrome Study Network (NEPTUNE),[39] (ii) eQTL in tubulointerstitial tissue from Susztak data,[40] and (iii) eQTL in kidney cortex tissue from the Genotype-Tissue Expression (GTEx) project.[41] For genes within genome-wide significant eGFR-associated loci, we evaluated whether the respective eQTLs were previously described as credible set variants,[38] which means that they are statistically more likely causal for the respective eGFR association signal than other variants in the same genetic locus.

Protein-protein interaction network

The molecular network analysis on the 5 known ADTKD genes and the 27 selected candidate genes was performed using the Search Tool for Retrieval of Interacting Genes/Proteins (STRING v11.5) database (https://string-db.org/).[42] A comprehensive network was built up from known and predicted associations, with confidence scores from 0.15 to 0.4, indicating the strength of data support.

RESULTS

Patient recruitment and initial genetic analysis

Patients were either recruited locally or referred by attending nephrologists throughout Germany. Only patients and their families were eligible who fulfilled the clinical KDIGO criteria for ADTKD[7] (in essence, CKD with bland urinary sediment, no to moderate proteinuria, and normal or decreased size kidneys), with their pedigree consisting of at least 2 affected family members in 2 successive generations. Each individual

Table 2 | ADTKD families with their respective mutation

Family ID	Index patient ID	Gene	cDNA	Amino acid
A-5	ADTKD-0003	*MUC1*	c.428dupC	MUC1-fs
A-11	ADTKD-0013	*MUC1*	c.428dupC	MUC1-fs
A-12	ADTKD-0015	*MUC1*	c.428dupC	MUC1-fs
A-14	ADTKD-0017	*MUC1*	c.428dupC	MUC1-fs
A-15	ADTKD-0018	*MUC1*	c.428dupC	MUC1-fs
A-21	ADTKD-0024	*MUC1*	c.428dupC	MUC1-fs
A-23	ADTKD-0026	*MUC1*	c.428dupC	MUC1-fs
A-24	ADTKD-0027	*MUC1*	c.428dupC	MUC1-fs
A-29	ADTKD-0032	*MUC1*	c.428dupC	MUC1-fs
A-30	ADTKD-0041	*MUC1*	c.428dupC	MUC1-fs
A-33	ADTKD-0048	*MUC1*	c.428dupC	MUC1-fs
A-35	ADTKD-0055	*MUC1*	c.428dupC	MUC1-fs
A-36	ADTKD-0056	*MUC1*	c.428dupC	MUC1-fs
A-37	ADTKD-0057	*MUC1*	c.428dupC	MUC1-fs
A-38	ADTKD-0058	*MUC1*	c.428dupC	MUC1-fs
A-43	ADTKD-0070	*MUC1*	c.428dupC	MUC1-fs
A-47	ADTKD-0077	*MUC1*	c.428dupC	MUC1-fs
A-50	ADTKD-0082	*MUC1*	c.428dupC	MUC1-fs
A-59	ADTKD-0106	*MUC1*	c.428dupC	MUC1-fs
A-6	ADTKD-0006	*UMOD*	c.397_405del	p.(Tyr133_Cys135del)
A-13	ADTKD-0016	*UMOD*	c.586G>A[43]	p.(Asp196Asn)
A-16	ADTKD-0019	*UMOD*	c.707C>G[44]	p.(Pro236Arg)
A-27	ADTKD-0030	*UMOD*	c.768C>G	p.(Cys256Trp)
A-32	ADTKD-0047	*UMOD*	c.509G>A[45]	p.(Cys170Tyr)
A-41	ADTKD-0066	*UMOD*	c.1463G>A[46]	p.(Gly488Asp)
A-44	ADTKD-0072	*UMOD*	c.899G>T	p.(Cys300Phe)
A-61	ADTKD-0132	*UMOD*	c.(464G>A; 907G>C)	p.(Cys155Tyr; Asp303His)
A-18	ADTKD-0021	*HNF1B*	c.780G>C[47]	p.(Glu260Asp)
A-10	ADTKD-0012	*REN*	c.45_47del[14]	p.(Leu16del)

ADTKD, autosomal dominant tubulointerstitial kidney disease; ID, identifier; MUC1-fs, mucin 1 frameshift protein.
Part of this cohort was previously published in Ekici *et al.*,[21] Wenzel *et al.*,[27] and Knaup *et al.*[16] Initial reports of individual mutations are cited (Williams *et al.*,[43] Sanna-Cherchi *et al.*,[44] Dahan *et al.*,[45] Bokhove *et al.*,[46] So *et al.*[47]). c.428dupC of *MUC1* was reported in Kirby *et al.*[12] In family A-61, the 2 variants lie in *cis*, as confirmed by segregation in successive generations.

(affected or nonaffected) signed the informed consent and was assigned a pseudonym (ADTKD-0xxx), which was entered into the pedigrees. Initially, all index patients were primarily tested for the 5 known genes for ADTKD and the common dupC mutation of *MUC1* by SNaPshot PCR.[21] If also negative, the families were classed as ADTKD-NOS, and an exome-wide approach was initiated. In parallel, the pedigrees of these families were checked for compatibility with mitochondrial inheritance, and a histologic screen was undertaken for atypical *MUC1* mutations, wherever possible (Figure 1). Genotyping for segregation of variants was always undertaken on every individual with a pseudonym in ADTKD-NOS families.

Figure 1 shows the results of the sequencing analysis of the 5 known ADTKD genes in 45 families. In 29 families, a diagnostic mutation was identified, with the most frequent subtype being *MUC1* (42% [19 of 45]), followed by *UMOD* (18% [8 of 45]), *HNF1B* (2% [1 of 45]), and *REN* (2% [1 of 45]). Mutations in *SEC61A1* were not identified (Table 2[12,16,21,27]). A total of 16 ADTKD-NOS families (36%) were identified (see Supplementary Clinical Notes for detailed clinical description and pedigrees). Table 3 summarizes the clinical data and characteristics of these families. More important, the phenotype of the ADTKD-NOS families does not show a notable difference in comparison to the specified ADTKD families or the KDIGO criteria.[7] Thereby, a typical difficulty is already displayed, because in many cases biopsies or ESRD of investigated patients has taken place many years or even decades ago. This circumstance handicaps the quality of the data but is a real-life situation in clinical nephrology.

Extended genetic analysis in ADTKD-NOS families

We next performed the *nephrome* analysis of these 16 ADTKD-NOS families, which yielded 10 diagnostic mutations in 9 families, segregating with the disease status in their respective families. Rather unexpectedly, most of the affected genes are traditionally considered to be involved in glomerular diseases: collagen IV–associated diseases or Alport syndrome (AS; 4× *COL4A5* [OMIM number 301050]; 1× *COL4A4* [OMIM number 203780]), focal segmental glomerular sclerosis (FSGS) type 7 (*PAX2* [OMIM number 616002]), and 2× FSGS type 5 (*INF2* [OMIM number 613237]). Several variants were excluded by segregation, gene curation (*PKD1*), or lacking splice effect in mRNA extracted from patient-derived skin fibroblasts (*FN1*). Table 4[21,48] lists all of the detected variants from the *nephrome* analysis and the conclusions drawn by specific criteria. The classic and atypical features of respective index patients in these families are summarized in Supplementary Table S2. The predicted effect of each missense variant of *COL4A5* and *INF2* is depicted in Supplementary Figure S1. Furthermore, the effects of the copy number variants for *PAX2*, *SALL1*, and *PKD2*, as well as the splice site variant within *COL4A4*, are discussed in Supplementary Table S3.

Table 3 | ADTKD-NOS clinical characteristics

Family ID	Index patient ID	Affected individuals/ generation	Age at ESRD, yr	Kidney biopsy	Urinary findings (at CKD stage)	Renal imaging (ultrasound, at respective CKD stage)
A-1	ADTKD-0001	3/3	II.2 at 63 III.1* at 36	III.1*-2012 (only report)	Bland urinary sediment (G3a)	Hyperechogenic, normal size, no cysts
A-2	ADTKD-0102	5/2	II.2 at 60 III.3* at 42 III.4 at 34 III.6 at 45	No	Not available	Not available
A-7	ADTKD-0062	4/2	II.2 at 55 II.4 at 51 II.5 at 19 III.1* at 19	III.2-1989	Bland urinary sediment, proteinuria 2, 11 g/L (G4)	Decreased in size, no cysts
A-8	ADTKD-0010	4/3	I.1 at 67 II.2 at mid-50s II.3* at 56	No	Bland urinary sediment, proteinuria, 732 mg/L (G4)	Normal size 1 cyst left kidney ~2.1 cm
A-17	ADTKD-0020	4/2	II.1 at 36 III.1* at 23	No	Urine dipstick test protein (++), erythrocytes (+) (G5)	Decreased in size, no cysts
A-26	ADTKD-0029	4/2	II.3 at 29 III.2* at 58	III.2*-1996 (only report)	Bland urinary sediment (G3a)	Hyperechogenic, normal size, no cysts
A-31	ADTKD-0045	5/3	II.6 at 65 III.2* at 79	III.2*-2008	Bland urinary sediment, no proteinuria (G2)	Normal size, no cysts
A-42	ADTKD-0067	4/4	II.1 at 72 III.2* at 66 IV.2 at 11	No	Bland urinary sediment, proteinuria, 530 mg/L (G5)	Decreased in size, no cysts
A-48	ADTKD-0079	6/3	I.1 at 48 II.4* at 60	III.2-1994 (only report)	Bland urinary sediment, proteinuria, 1.31 g/L (G4)	Hyperechogenic, decreased in size, no cysts
A-49	ADTKD-0080	3/3	I.1 at 60 II.1* at 47	I.1-2014 II.1*-2018	Bland urinary sediment, moderate proteinuria, 1.4 g/L (G4)	Decreased size, no cysts
A-51	ADTKD-0085	7/4	II.1 at 80 II,3 at 73 III.3* at 52	No	Bland urinary sediment, proteinuria, 1.1 g/L (G5)	Decreased in size, left kidney one 0.5 × 0 × 4-cm cyst
A-52	ADTKD-0090	5/4	III.2 at 66 IV.2* at 37	IV.2*- 1980 (no report + no material)	Not available	Not available
A-53	ADTKD-0091	7/2	II.2 at 67 II.4 at 78 II.6 at 66 II.5 at 60 III.6 at 62	III.6-2011 III.7*-2019	Bland urinary sediment, proteinuria, 150 mg/L (G3)	Decreased size, no cysts
A-54	ADTKD-0092	4/3	None	No	Bland urinary sediment, proteinuria, 800 mg/L (G4)	Decreased size right side, 4–5 cysts up to 20 mm in size both sides
A-56	ADTKD-0094	3/2	II.5 at 17	III.2*-2011	Bland sediment, no proteinuria (G3a)	Normal size, no cysts
A-57	ADTKD-0095	7/2	I.2 at 41 II.1 at 42 II.3 at 36 II.7 at 42 II.9 at mid-20s II.11* at 49 II.15 at 36	No	Bland urinary sediment, proteinuria, 197 mg/L (G2)	Normal size, no cysts

ADTKD, autosomal dominant tubulointerstitial kidney disease; CKD, chronic kidney disease; ESRD, end-stage renal disease; ID, identifier; NOS, not otherwise specified. Affected individuals are defined as established CKD stage 3 or worse and/or detected familial mutation. Kidney biopsies where no biopsy material could be obtained have the addition: report only or no report. Marked individuals (roman and Arabic numbering) in columns 4 and 5 can be identified in the pedigrees provided (Figures and Supplementary document). Asterisks mark the index patients of the respective family. Urinary findings and renal imaging are provided from the respective index patient. Proteinuria can increase unspecifically over the progression of CKD, which is why the CKD stage is provided. Ultrasound findings reported date to the time frame (stage of CKD) of the urinary findings.

Table 4 | Genetic variants from *nephrome*

Family ID	Index patient ID	Variant	ACMG class	CADD score	Reason for exclusion	Diagnostic mutation
A-1	ADTKD-0001	**None**	—	—	—	—
A-2	ADTKD-0102	***COL4A5*** (NM_000495.4): exon 47: c.435G>T, p.(Gly1451Val), hemizygous	5	28.3	—	***COL4A5***
A-7	ADTKD-0062	***PAX2***: GRCh37/hg19: NC_000010.10: g.(?_102495466)_(102510648_?)dup	4	N/A	—	***PAX2***
A-8	ADTKD-0010	**None**	—	—	—	—
A-17	ADTKD-0020	***INF2*** (NM_22489.3): exon 6: c.764G>A, p.(Asp255Asn), heterozygous	3	27.1	—	***INF2***
A-26	ADTKD-0029	***INF2*** (NM_22489.3): exon 2: c.212A>C, p.(Gln71Pro), heterozygous	4	21.4	—	***INF2***
A-31	ADTKD-0045	**None***	—	—	—	—
A-42	ADTKD-0067	***FN1*** (NM_002026.2): intron 22: c.3518-3T>C, heterozygous	3	9.1	No splice effect	—
A-48	ADTKD-0079	***COL4A5*** (NM_000495.4) exon 25: c.1871G>A, p.(Gly624Asp)	5	24.6	—	***COL4A5***
A-49	ADTKD-0080	***COL4A4*** (NM_000092.4): intron 45: c.4333+2T>C, heterozygous	4	26.9	—	***COL4A4***
		PKD1 (NM_000296.3): exon 15: c.4057G>A, p.(Gly1353Ser), heterozygous	3	25	Gene curation	—
A-51	ADTKD-0085	***COL4A5*** (NM_000495.4) exon 25: c.1871G>A, p.(Gly624Asp), hemizygous	5	24.6	—	***COL4A5***
A-52	ADTKD-0090	***COL4A5*** (NM_000495.4) exon 51: c.5030G>A, p.(Arg1677Gln), hemizygous	5	33	—	***COL4A5***
A-53	ADTKD-0091	***SLC7A9*** (NM_014270.4): exon 5: c.544G>A, p.(Ala182Thr), heterozygous	4	15.73	Segregation	—
A-54	ADTKD-0092	***SALL1*** (NM_001127892): genomic, heterozygous deletion around exon 2 and 3'UTR: HGVS: NC_000016.9: g.(?_51168112)_(51171538_?)del	4	N/A	—	***SALL1***
		PKD2 (NM_000297): genomic, heterozygous deletion of exon 13: HGVS: NC_000004.11: g.88989050-88989213del, r. 2458_2621del, p.Leu842ProfsTer20	4	N/A	—	***PKD2***
A-56	ADTKD-0094	***COL4A3*** (NM_000091.49): exon 23: c.1483C>T, p.(His495Tyr), heterozygous	3	15.02	Segregation	—
		BLK (NM_001715.2): exon 11: c.1075C>T, p.(Arg359Cys), heterozygous	3	29.4	Segregation	—
A-57	ADTKD-0095	GRCh37/hg19: heterozygous deletion NC_000020.10:g.(?_62669975)_(62694737_?) Deleted genes: ***C20orf204***, ***SOX18***, ***TCEA2***	3	N/A	Segregation	—
		EHHADH (NM_001966.3): exon 7: c.1411G>C, p.(Val471Leu), heterozygous	3	25.3	Segregation	—

ACMG, American College of Medical Genetics and Genomics; ADTKD, autosomal dominant tubulointerstitial kidney disease; CADD, Combined Annotation Dependent Depletion; HGVS, Human Genome Variation Society; ID, identifier; N/A, not applicable; UTR, untranslated region.
The genetic variants of individual families identified in the *nephrome* with their exact position in relation to the accession number provided. The variant classification by ACMG and the evaluation by the CADD score are displayed (see Methods section). Asterisk in family A-31 marks the segregating *UMOD* T62P variant, which was already reported in Ekici *et al.*[21] and further studied in Olinger *et al.*[48] Structural impacts of *COL4A5* and *INF2* missense mutations are shown in Supplementary Figure S1. See Supplementary Table S3 for further validation of the diagnostic copy number variants (*PAX2*, *SALL1*, and *PKD2*) and the splice site variant in *COL4A4*. For better visualization, the predominant findings per family are highlighted in bold. CADD scores do not describe copy number variants and, therefore, are indicated as N/A. Dashes were placed where no entry was possible.

Phenotype reanalysis of individual families

The families with a classically considered glomerular origin of their disease were thoroughly reanalyzed for the existing clinical data wherever possible to ensure that crucial information was not overlooked when classifying them as ADTKD. The index patient in family A-7 showed a paternally inherited duplication commencing in the 5′-untranslated region and spanning the exons 1 to 3 in the *PAX2* gene (Figure 2a and b). *PAX2* (paired box 2) is a transcription factor with a critical role in the development of the urogenital tract, the eyes, and the central nervous system. Mutations in the *PAX2* gene are known to cause

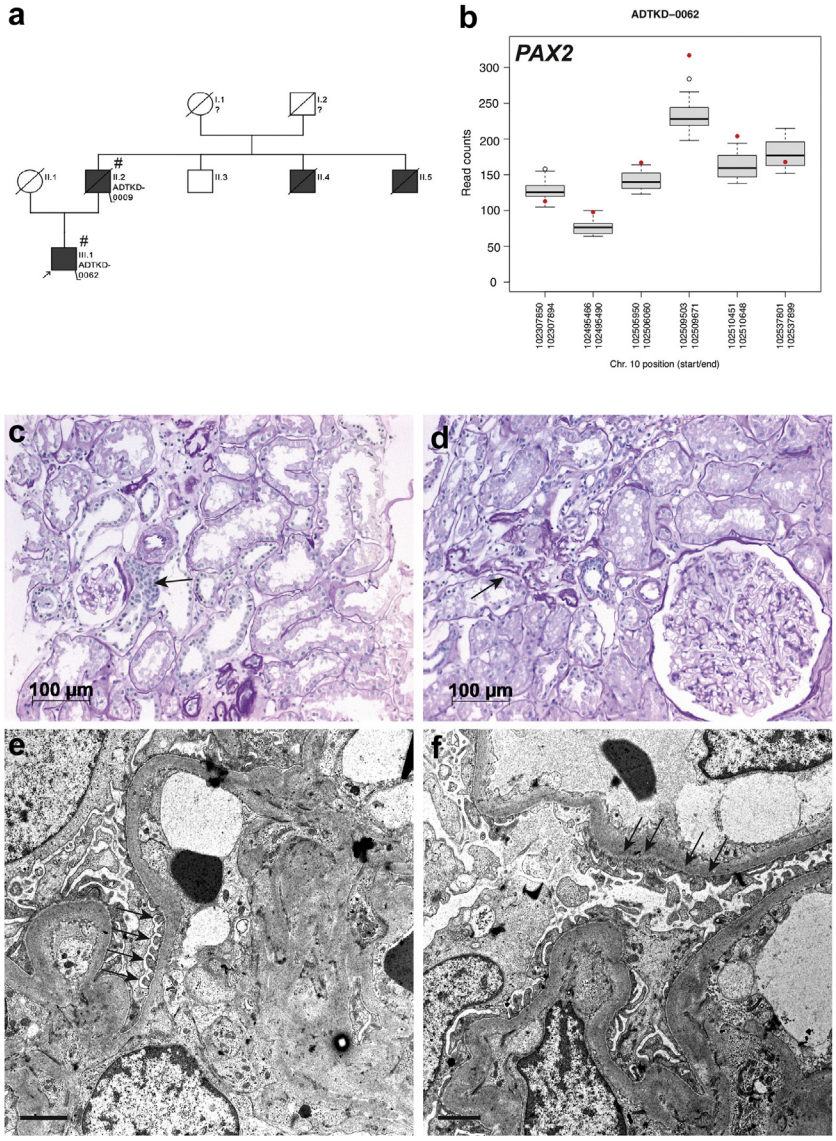

Figure 2 | Features and consequences of an identified *PAX2* mutation. Pedigree of family A-7 (**a**), displaying 4 affected individuals, all experiencing end-stage renal disease, in 2 generations, including the index patient autosomal dominant tubulointerstitial kidney disease (ADTKD)–0062 (arrow). The existing information did not reliably enable identification of the affected individual in generation I, who was deceased (for more information, see Table 3 and Supplementary Clinical Notes). Circles symbolize female individuals, and squares symbolize male individuals. Filled (black) symbols mark affected family members. #Individual who was analyzed by next-generation sequencing. (**b**) Visualization of copy number variant analysis in the index patient ADTKD-0062, showing a duplication commencing within the 5′-untranslated region (UTR) and spanning from exon 1 to exon 3 of the *PAX2* gene. Box and red dot plots of read counts (*y* axis) are shown as identified by ExomeDepth for individual ADTKD-0062 (red dot) and all nonrelated exomes in the same run ($n = 46$; box) and white dots as outliers (control) for the different exome targets of the *PAX2* gene on chromosome (Chr.) 10 (*x* axis; 5′-UTR: 102495466–102495490; exon 1: 102505950–102506060; exon 2: 102509503–102509671; exon 3: 102510451–102510648). An equivalent data set was achieved by analyzing the stored DNA of the index patient's father (ADTKD-0009; data not shown). (**c,d**) Light microscopy of a kidney biopsy of individual ADTKD-0009 at the age of 34 years in 1989 (II.2), illustrating mild interstitial fibrosis/tubular atrophy (arrow in **d**) and focal lymphocytic infiltration (arrow in **c**). Glomeruli appear normal on light microscopy (**d**). Routine immunohistochemistry was negative (data not shown). Bars indicate the magnification. Sections were stained with periodic acid–Schiff. (**e,f**) Electron microscopy, demonstrating mesangial matrix expansion and mild wrinkling of the glomerular basement membranes as well as predominantly well-preserved podocyte foot processes (arrows in **e**) with focal and mild effacement (arrows in **f**). Bars = 2000 nm. Thus, the biopsy report at the time described no seminal finding; in particular, no segmental glomerular sclerosis was observed. To optimize viewing of this image, please see the online version of this article at www.kidney-international.org.

FSGS type 7 (OMIM number 616002) and papillorenal syndrome (OMIM number 120330[49,50]). None of the affected family members were reported to have experienced nephrotic syndrome. The little information that could be found in the clinical archive is low to moderate proteinuria in the index patient. Ophthalmologic investigation did not show retinal coloboma. A single historical kidney biopsy within this family was taken >3 decades ago (Table 3) from

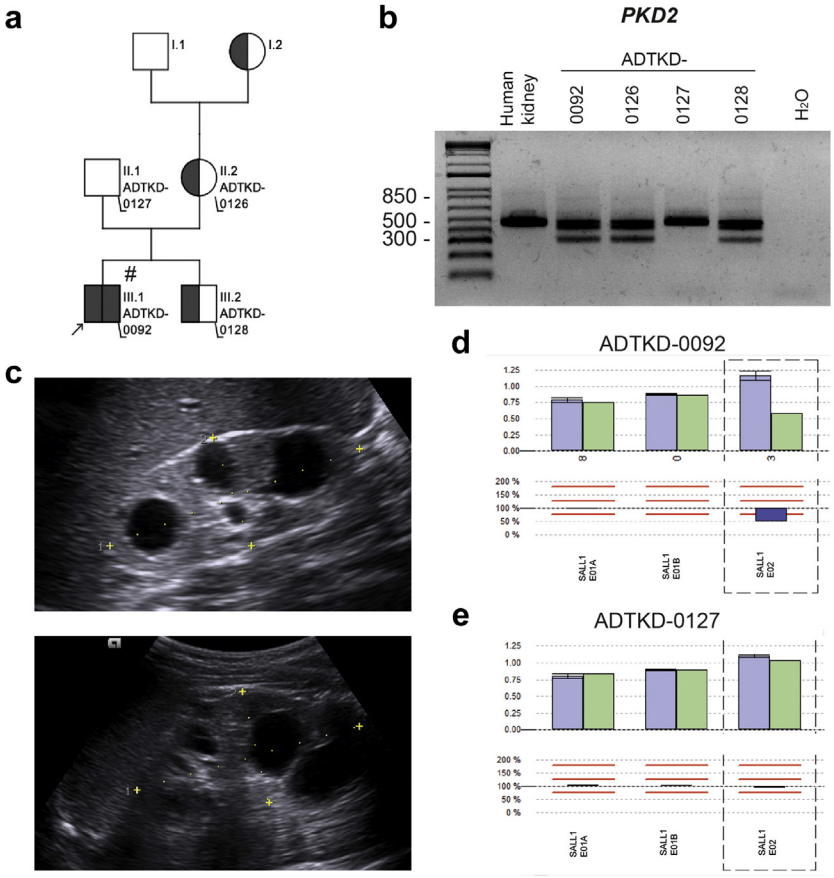

Figure 3 | Blended phenotype by a *de novo SALL1* and familial *PKD2* deletion. Pedigree of family A-54 (**a**), displaying 4 affected individuals in 3 generations, all experiencing autosomal dominant polycystic kidney disease on the basis of a *PKD2* deletion, symbolized by filled (black) half symbols on the left-hand side. #Individual who was analyzed by next-generation sequencing. The arrow indicates the index patient, autosomal dominant tubulointerstitial kidney disease (ADTKD)–0092. All affected members show numerous bilateral kidney cysts. To date, apart from the index patient, only the grandmother (I.2) shows chronic kidney disease (CKD; stage 3), next to several distant family members abroad with end-stage renal disease (for more information, see Supplementary Clinical Notes). (**b**) Agarose gel image of a polymerase chain reaction, specific for the exon 13 deletion of *PKD2* from the cDNA of all available family members (as indicated). Only the affected patients show an additional signal that migrates faster, at ≈300 bp, corresponding to the genomic deletion of the mutated allele. All samples amplify a signal at ≈450 bp from the wild-type allele, including a positive control from cDNA of healthy human kidney. Right-hand line marks the negative control with water instead of DNA. (**c**) Ultrasound images of the rather small kidneys of the index patient, ADTKD-0092, with CKD stage 4, showing several solitary cysts next to intact renal structures (upper panel showing right kidney with the dimensions [i] 76.8 mm and [ii] 32.9 mm; lower panel showing left kidney with the dimensions [i] 85.9 mm and [ii] 43.2 mm). Overall, the kidney cysts do not appear to sufficiently explain the progress of CKD in this patient. (**d,e**) Confirmation of *SALL1* exon 2 deletion by multiplex ligation-dependent probe amplification analysis in the affected patient. The upper histogram shows fluorescent intensity of amplification (*y* axis) of single exon (*x* axis) of the patient sample in green and of control samples in blue. The lower histogram shows the ratio of fluorescent intensity of amplification calculated from proband versus controls. If the ratio exceeds the defined limits indicated by the red lines, a dark blue bar indicates a genomic change. We used a lower limit (lower dotted line) of 75% (deletion) and an upper limit (higher dotted line) of 130% (duplication). Data are expressed as means ± SD of control samples. Only the index patient (ADTKD-0092) bares the exon 2 deletion of *SALL1*. Family members ADTKD-0126 and ADTKD-0128 showed an identical result like the nonaffected individual, ADTKD-0127 (data not shown).

the father of the index patient, which did not show glomerular pathology indicating FSGS (Figure 2c and d), but discrete interstitial fibrosis and tubular atrophy and minimal interstitial inflammatory infiltrates. More important, the electron microscopy did not show glomerular basement membrane pathology and predominantly intact podocytes with only focal podocyte foot process effacement (Figure 2e and f).

The index patient in family A-54 was referred for ADTKD diagnostics at the age of 27 years, showing CKD stage 4 without any sign of glomerular disease. Interestingly, the mother and grandmother were known to show numerous kidney cysts, and the grandmother had CKD stage 3 years ago (Figure 3a). Several relatives with ESRD after the sixth decade of life were reported but not available for genetic testing. The index patient showed several cysts in rather small kidneys, not explaining the extent of CKD (Figure 3c). The *nephrome* analysis showed a deletion of exon 13 in *PKD2* (Figure 3b) as well as a deletion of exon 2 in *SALL1* (Figure 3d and e). The *PKD2* deletion segregated within the affected family members, establishing the diagnosis of autosomal dominant polycystic kidney disease. However, the *SALL1* variant in the index patient was *de novo*. *SALL1* mutations have been reported previously to cause Townes-Brocks syndrome (OMIM

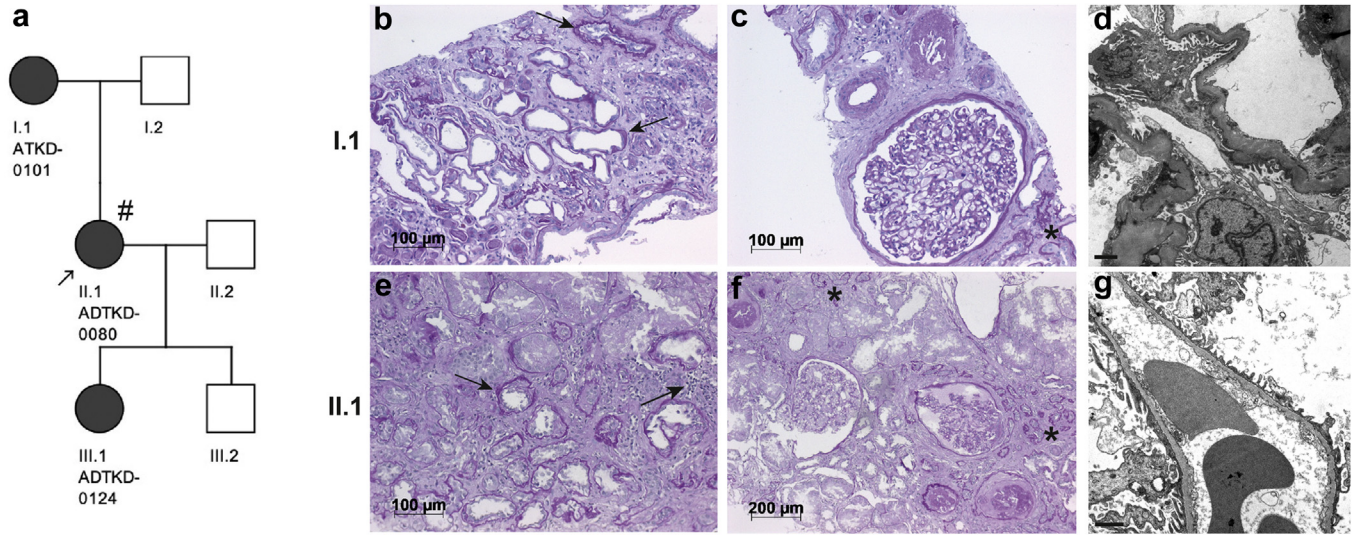

Figure 4 | Features and consequences of an identified *COL4A4* mutation. Pedigree of family A-49 (**a**), illustrating 3 affected individuals in 3 generations, including the index patient, autosomal dominant tubulointerstitial kidney disease (ADTKD)-0080 (arrow). #Individual who was analyzed by next-generation sequencing. The index patient and her mother, ADTKD-0101, have end-stage renal disease, whereas the daughter, ADTKD-0124, shows persistent microhematuria with currently normal glomerular filtration rate and no proteinuria at the age of 26 years (for more information, see Table 3 and Supplementary Clinical Notes). Light microscopy of historic kidney biopsies (**b**,**c**,**e**,**f**) of the index patient and her mother, illustrating pronounced interstitial fibrosis/tubular atrophy (asterisks in **c**,**f**) with lymphocytic infiltration and lamellation of tubular basement membranes (arrows in **b**,**e**). Glomeruli show uncharacteristic changes (**c**,**f**), with advanced global sclerosis, as depicted in the index patient (**f**). Routine immunohistochemistry was negative (data not shown). Bars indicate the magnification. Sections were stained with periodic acid–Schiff. (**d**,**g**) Electron microscopy, demonstrating wrinkling of the glomerular basement membranes and only mild foot process effacement compatible with mild ischemic injury in patient ADTKD-0101 without textural changes of the basement membranes (**d**) and thinning of the glomerular basement membranes (mean width, 151 nm) in patient ADTKD-0080 (**g**). Thus, thin basement membrane disease was discussed. Bars = 2000 nm. To optimize viewing of this image, please see the online version of this article at www.kidney-international.org.

number 107480), variably associated with malformations of multiple organ systems (eyes, ears, anal and genitourinary tract, kidneys, and heart) and extremities, as well as functional renal impairment leading to ESRD.[51] Therefore, the digenic nature of findings in the index patient may explain the increased severity of his phenotype, compared with his affected relatives, in a blended phenotype.[52] Interestingly, the index patient had to undergo surgery for anal stenosis and

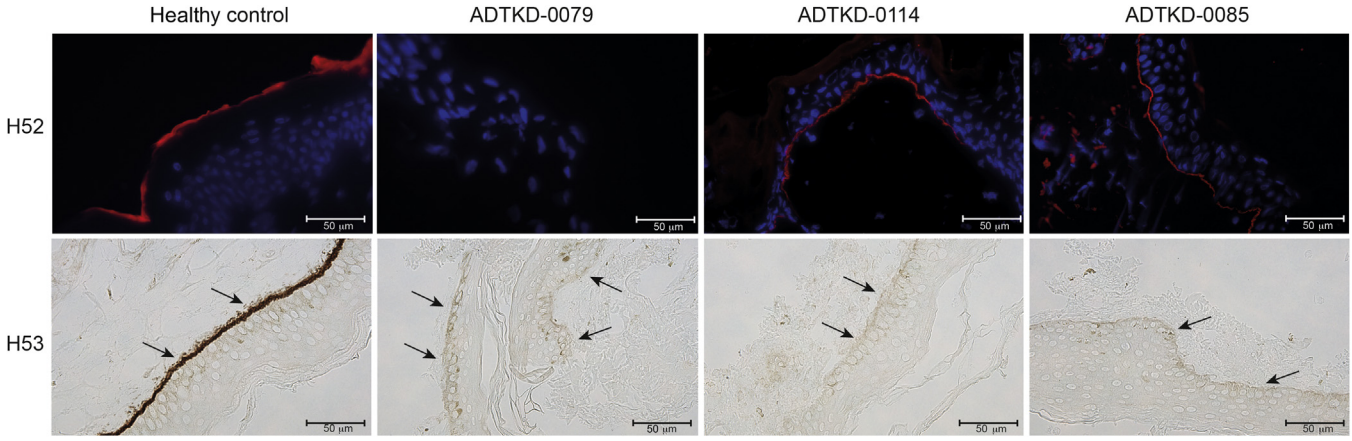

Figure 5 | Immunohistochemical detection of type IV collagen chain α5 (Col α5[IV]) in skin biopsies from patients with the p.(Gly624Asp) mutation. Skin biopsies from a healthy control (left-hand panels) and 3 affected individuals were compared by immunofluorescence (IF) with the anti–Col α5(IV) antibody H52 (upper panel) and by immunohistochemistry with the antibody H53 (lower panel), detecting distinct epitopes. One hemizygous male patient (autosomal dominant tubulointerstitial kidney disease [ADTKD]–0085) was analyzed in parallel to 2 heterozygous women (ADTKD-0079 and ADTKD-0114). Both antibodies detect Col α5(IV) in the dermal basement membrane of healthy controls, whereas the H53 antibody does not detect the protein in any patient. However, H52 detects Col α5(IV) in 2 patients but not in the female ADTKD-0079. Arrows indicate the position of the dermal basement membrane, where the Col α5(IV) protein should be located. Bars indicate the magnifications used. Nuclei were counterstained in IF with 4′,6-diamidino-2-phenylindole. To optimize viewing of this image, please see the online version of this article at www.kidney-international.org.

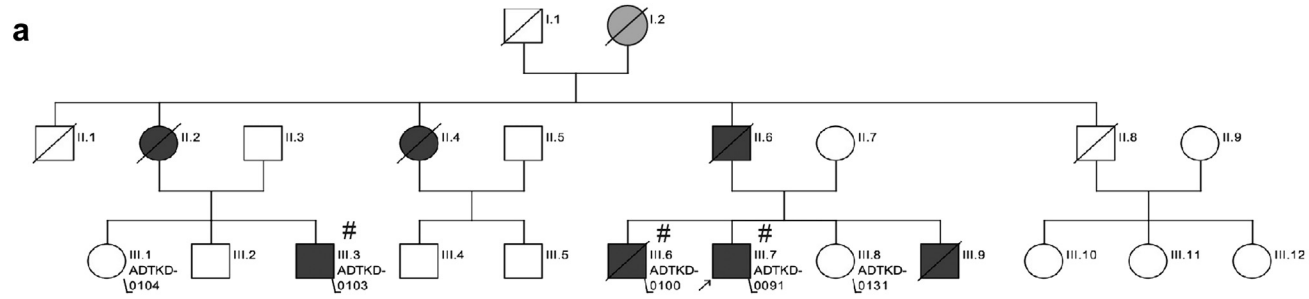

Family ID	Gene	Position	cDNA	Amino acid	AA conservation	Polyphen2 /SIFT	CADD	Allele frequency gnomAD	ClinVar
A-53	*HELZ2*	chr20:62192526 A>G	c.7055T>C	p.(Leu2352Pro)	+	P / 0.01	23.79	Variant not found	Not reported
	ITPRIPL2	chr16:19126288 C>T	c.505C>T	p.(Arg169Cys)	–	D / 0.09	25	Variant not found	Not reported
	JMJD6	chr17:74721921 G>T	c.146C>A	p.(Ala49Glu)	+	P / 0.14	20.2	0/5/246434	Not reported
	WNT11	chr11:75905687 G>A	c.521C>T	p.(Ala174Val)	++	D / 0.16	24.79	Variant not found	Not reported

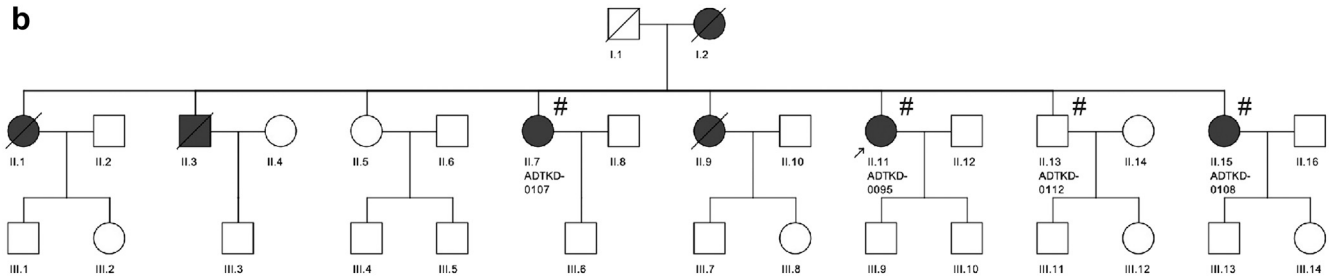

Family ID	Gene	Position	cDNA	Amino acid	AA conservation	Polyphen2 /SIFT	CADD	Allele frequency gnomAD	ClinVar
A-57	*CHI3L1**	chr1:203154410G>C	c.159C>G	p.(His53Gln)	++	D / 0	22.9	Variant not found	Not reported
	FBXO18	chr10:5955754C>T	c.1409C>T	p.(Ser470Phe)	+	D / 0.01	25.6	Variant not found	Not reported
	*PLEKHM1**	chr17:43522860C>A	c.2813G>T	p.(Gly938Val)	++	D / 0.1	25	Variant not found	Not reported

Figure 6 | Clinical findings and exome analysis of families A-53 and A-57. Pedigree of family A-53 (**a**), illustrating 7 affected individuals (6× end-stage renal disease [ESRD], and 1× chronic kidney disease G5) in 2 generations, including the index patient autosomal dominant tubulointerstitial kidney disease (ADTKD)-0091 (arrow). #Individuals who were analyzed by next-generation sequencing (NGS). The grandmother (I.2) of the index patient died early in the fourth decade of life and was believed to have kidney disease (symbol in pedigree in gray, because information is not fully resilient; for more information, see Table 3 and Supplementary Clinical Notes). Pedigree of family A-57 (**b**), illustrating 7 affected individuals (all with ESRD) in 2 generations, including the index patient ADTKD-0095; arrow). For more information, see Table 3 and Supplementary Clinical Notes. #Individuals who were analyzed by NGS. Because the pedigree is principally compatible with mitochondrial inheritance, we also analyzed mitochondrial DNA, which did not yield a diagnostic variant. The list beneath the respective family pedigree shows results of *in silico* analysis of selected variants in 4 candidate genes (A-53), with 3 candidate genes (A-57) that have fulfilled the filtering criteria (see Methods) and segregate with disease status in those family members who have been assigned a patient identifier (ID). Conservation of amino acids (not conserved [–], moderately conserved [+], to highly conserved [++]). Variants with a (continued)

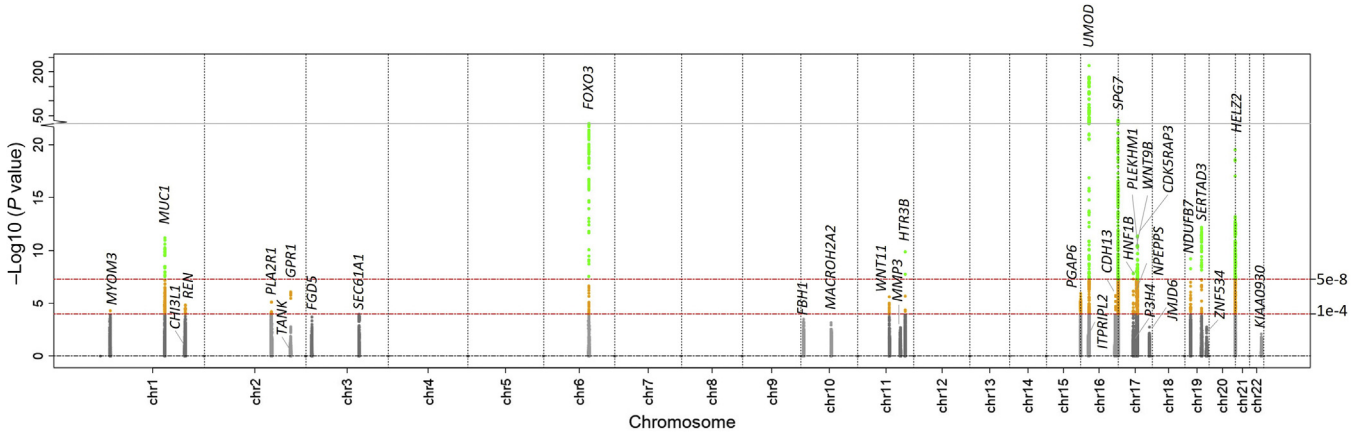

Figure 7 | Association of genetic regions around known and identified autosomal dominant tubulointerstitial kidney disease (ADTKD) genes with estimated glomerular filtration rate (eGFR) in general populations. We queried the regions around the 5 known and 27 potentially novel genes for ADTKD (gene region ± 250 kb) for association with eGFR from genome-wide association study meta-analysis (n = 1,202,929; Stanzick *et al.*[38]). Shown are association P values on the $\log_{10}$ scale by chromosomal base position (GRCh37) reduced to the relevant gene regions. The red dashed lines mark genome-wide significant and suggestive association (5×10^{-8} or 1×10^{-4}, respectively). Green and orange dots mark single-nucleotide polymorphisms that reach genome-wide significant or suggestive association, respectively. Chr, chromosome.

hypospadia as a newborn. In addition, the patient shows a hypoplastic right thumb (Supplementary Clinical Notes and Supplementary Figure S19), in summary establishing the diagnosis of Townes-Brocks syndrome.

In agreement with other studies, we identified several families with AS, which appears to be much more frequent than clinically anticipated.[4,53,54] We identified a *COL4A4* variant in family A-49, which segregated with disease state in 3 generations (Figure 4a). Neither of the 2 existing kidney biopsies showed glomerular basement membrane changes diagnostic for AS. Reanalysis of these biopsies showed rather unspecific tubulointerstitial fibrosis (Figure 4b and e), as well as pronounced glomerulosclerosis (Figure 4c and f). More important, the electron microscopy of both biopsies also did not show findings diagnostic for AS (Figure 4d and g), although thinning of glomerular basement membrane was noted in the index patient, ADTKD-0080 (Figure 4g). The families A-2, A-48, A-51, and A-52 are affected by a mutation in *COL4A5* (Table 4 and Supplementary Figure S1). Interestingly, 2 of these families (A-48 and A-51) show the recently reported "hypomorphic" mutation c.1871G>A (p.[Gly624Asp]), which appears to be a founder mutation in central Europe, leading to a relatively mild disease and usually reaching ESRD in mid adulthood.[55,56] Because skin biopsies are often discussed as additional diagnostic option in AS,[57] we were particularly interested in the findings of this frequent mutation. Figure 5 shows the results of immunostaining with 2 different antibodies against type IV collagen chain α5 (Col α5[IV]) on skin biopsies, where in our hands the antibody H52 only functions in cryopreserved immunofluorescence and H53 only in paraformaldehyde-fixed and embedded biopsies in immunohistochemistry. Interestingly, using the H53 antibody, none of the patients analyzed showed a specific signal for Col α5(IV). However, using the H52 antibody, the affected individuals ADTKD-0114 (female, heterozygote for the mutation) and ADTKD-0085 (male, hemizygote) show a specific signal along the dermal basement membrane, comparable to the control. The female patient ADTKD-0079 did not show staining with the H52 antibody. Because this finding is unexpected compared with the other 2 patients investigated, we analyzed the ES data for mutations in *COL4A1*, *COL4A2*, and *COL4A6*, which are also contained in the 3-dimensional molecule of collagen IV in the skin.[58,59] We could not identify any variant in these genes in patient ADTKD-0079. Furthermore, using DNA from the patient`s peripheral blood, we could not detect skewed X-inactivation, which might explain this unexpected result (data not shown). In summary, the staining results of the skin in patients with the *COL4A5* mutation p.(Gly624Asp) are difficult to interpret, and caution should be taken to use these data alone for clinical decision making and counseling.

Mitochondrial sequencing and ES, as well as search for atypical *MUC1* mutations in unsolved families

In 7 families, the *nephrome* analysis did not yield a putative disease-causing variant. The pedigrees of 3 families (A-1, A-56, and A-57) were compatible with mitochondrial

Figure 6 | (continued) damaging (D/0) or probably damaging (P/0.5-0) prediction effect based on 1 of at least 2 (Polyphen2/The Sorting Intolerant From Tolerant algorithm [SIFT]; see Methods) used prediction programs and with Combined Annotation Dependent Depletion (CADD) score >15 are shown. Allele frequency is based on the Genome Aggregation Database (gnomAD). None of the listed variants in the novel candidate genes are reported in Clinical significance of Variants (ClinVar) database. Asterisks mark genes that have been previously reported in a different genetic context with heterozygous variants. Chr, chromosome; D, damaging prediction effort; P, probably damaging prediction effort.

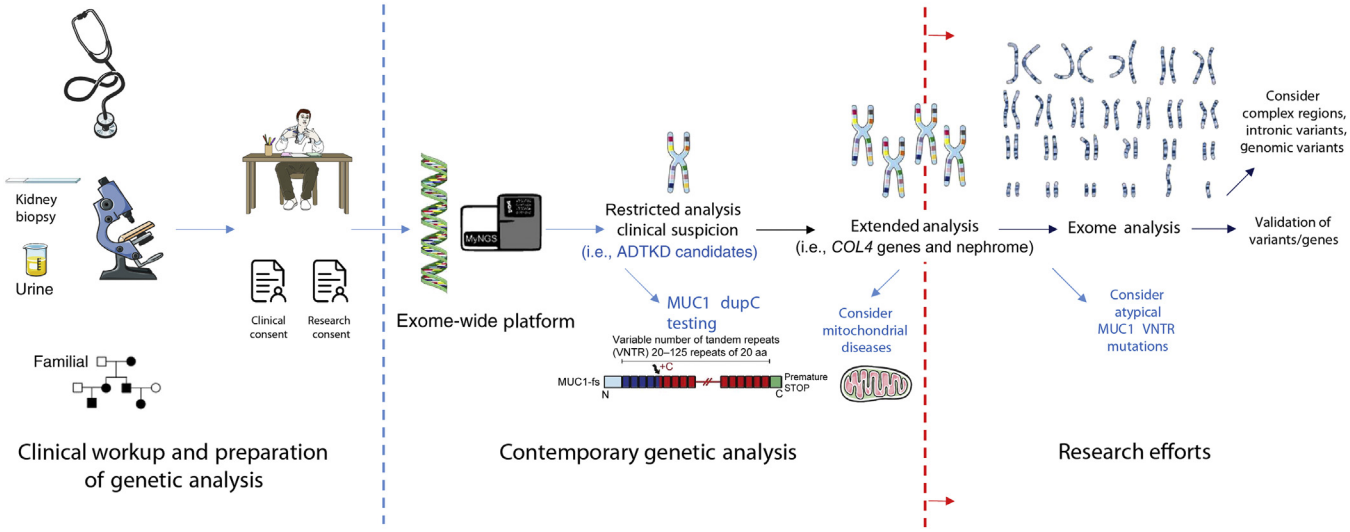

Figure 8 | Scheme of suggested diagnostic workflow for hereditary tubulointerstitial kidney diseases. Evaluation of a patient with the suspicion of a hereditary tubulointerstitial kidney disease starts with a thorough paraclinical/clinical assessment, possibly recognition of syndromic features, evaluation of urine parameters and kidney histology (if available), and careful pedigree analysis. These efforts should formulate a clinical suspicion for further genetic analysis, if the patient wishes to proceed. In prospect of potentially required broadening of the molecular diagnostics, we would recommend including research-based investigations in the primary patient consenting (left-hand panel of the scheme). For genetic analysis, we would meanwhile recommend using an exome-wide next-generation sequencing platform from the beginning, with stepwise extension of the genetic assessment, if no diagnostic variants can be detected. For autosomal dominant tubulointerstitial kidney disease (ADTKD) primarily, the 5 known genes should be studied, followed by the *MUC1* VNTR dupC mutation. If negative, the genetic analysis should be extended to further plausible genes, such as collagen IV genes (α3, 4, and 5), autosomal dominant focal segmental glomerular sclerosis disease candidates, and possibly the mitochondrial genome (should the pedigree show compatibility). All these steps would be desirable on a routine basis in a contemporary genetic analysis (middle panel). The borders toward research-based analyses (red dotted line) are variable, center dependent, and clearly conditional on staff (financial) resources. Therefore, investigation of the complete *nephrome* will only be possible in dedicated institutions on a routine basis. In present time, analysis of the exome is a research effort and has numerous implications for further validation steps. We would expect that the borders between routine and research analyses will be progressively shifted in future (red arrows on dotted line). In the context of tubulointerstitial diseases, atypical *MUC1* mutations could be considered. However, the detection of these are highly complex and clearly a research effort by specialized centers. The workflow indicates putative diagnostic steps for ADTKD/tubulointerstitial diseases with blue arrows and writing and the running changeover to other or unknown kidney diseases in black.

inheritance and, thus, were also analyzed for mitochondrially inherited tubulointerstitial kidney disease, which did not show a diagnostic variant (data not shown). Wherever available, kidney biopsies of these families were stained for mucin 1 frameshift protein,[16] and single-molecule, real-time sequencing was performed to sequence the Variable Number of Tandem Repeats (VNTR)[27] (Figure 1). The former did not detect mucin 1 frameshift protein (data not shown), and the latter merely showed wild-type VNTRs (Supplementary Table S4). The families were then taken on to an ES analysis, where minimally 1 and maximally 6 individuals per family were available for this analysis. In family A-8, only the index patient was available for analysis, thus resulting in 104 detected variants after ES, being too large for a meaningful conclusion (data not shown; available on request). The Supplementary Table S5 lists the results for candidate genes from the ES analysis of 4 families, who fulfilled the selection criteria (see Methods) and segregated with disease status within the families. Interestingly, not a single candidate gene was identified twice in the 7 families. Figure 6 shows exemplarily the results from these studies for individual families A-53 (Figure 6a) and A-57 (Figure 6b), including their respective pedigree depicting the number of affected family members and a list of segregating variants detected in 4 (A-53) and 3 (A-57) candidate genes.

Finally, we aimed to validate and prioritize the identified candidate genes. First, we queried the 5 known and 27 potentially novel ADTKD genes for evidence in recently published genome-wide association study data.[38] For 3 of the 5 known ADTKD genes (*UMOD*, *MUC1*, and *HNF1B*) and 9 of the 27 potentially novel ADTKD genes, the gene regions ± 250 kb contained at least 1 genome-wide significant variant associated with eGFR ($P < 5 \times 10^{-8}$; i.e., a known locus for eGFR; Figure 7[38]). We observed significant eQTLs (false discovery rate, <0.05) in kidney tissue for genes with genome-wide significant evidence for eGFR association for the 2 known ADTKD genes (*UMOD* and *MUC1*) and for 7 potentially novel ADTKD genes (*SPG7*, *SERTAD3*, *CDK5RAP3*, *HTR3B*, *NDUFB7*, *WNT9B*, and *PLEKHM1*; Supplementary Table S6). Among genes in regions with suggestive evidence for eGFR association, we found eQTLs in kidney tissue for further 6 potentially novel ADTKD genes (*GPR1*, *PGAP6*, *CDH13*, *WNT11*, *PLA2R1*, and *MYOM3*). Second, we performed numerous database analyses for association with animal models, protein function, and renal expression as well as searched for the identified alleles of the

27 candidate genes in the Genomics England 100,000 Genomes Project, which resulted in 2 hits connected to a kidney phenotype within *MMP3* and *CDK5RAP3* (Supplementary Table S7). Third, a STRING search of all known ADTKD candidate genes with the 27 identified exome variants showed a cluster of some candidates with the ADTKD genes (Supplementary Figure S2). With all due care, validation of the identified candidate genes by the different measures applied may prioritize the genes *FOXO3*, *MMP3*, *CDK5RAP3*, *WNT9B*, and *WNT11* for further functional analyses.

DISCUSSION

Recent data have shown that hereditary kidney diseases are more frequent than the clinical perception.[60] Thus, many families are still undiagnosed, although they may show a positive family history for kidney disease, which may date back for many generations. This situation is clearly unsatisfactory, considering the technological possibilities that are available nowadays. Large studies show that up to 30% of patients with ESRD may have a close family member also experiencing CKD, which demonstrates a strong genetic background in the population of patients with CKD,[61,62] although not all of these families will be affected by a monogenic disease. In patients suggestive of hereditary kidney disease, a genetic clarification is desirable for many reasons (i.e., contemporary and noninvasive conclusion of a diagnosis, family counseling, prevention of unnecessary therapeutic attempts, and access to targeted therapies or clinical studies, if available). Thus, modern nephrology should strive to correctly diagnose every single family with a hereditary trait.

Considering the clinical difficulties in recognizing patients with ADTKD, it is noteworthy that two-thirds of the families investigated herein were correctly placed into this disease entity (Figure 1). These numbers are comparable to other studies (summarized in Table 1). Therefore, the criteria developed to classify ADTKD[7] appear valid. Attempting to clarify the molecular cause of disease in the group of ADTKD-NOS will inevitably unravel incorrect clinical diagnoses (if a diagnostic variant in a gene is found, which was previously not anticipated) or identify novel candidate genes for ADTKD. The former was achieved in 9 families (Table 4), whereas the latter may be true for 7 families (Figure 6 and Supplementary Table S5). Rather unexpectedly, 8 of the 10 diagnostic variants (in 9 families) involve genes in a traditional context to glomerular diseases. This shows that clinical classification may be difficult, partly because of incomplete clinical information and partly because of atypical clinical course. In this context, it is tempting to speculate that some of the atypical clinical presentations may be caused by renal tubular pathomechanisms, not yet defined. Interestingly, the type IV collagen chains α3, 4, and 5 are also strongly expressed in the distal tubular basement membranes of the kidney.[59] However, its roles in physiology and diseases are not yet defined. Therefore, even the seemingly easy clinical differentiation between glomerular and tubulointerstitial disease may be blurry or faulty. For this reason, the best effort of clinical characterization of any given disease should be undertaken and the option for a broader successive genetic analysis should be reserved (see below).

In view of the recent results of next-generation sequencing analysis in representative CKD populations,[4,53,63] it is not surprising that collagen IV–associated diseases were the largest group of diagnoses among the ADTKD-NOS families (5 collagen IV–associated diseases; Table 4). In the past, collagen IV–associated diseases were reported to have been misclassified as hereditary FSGS in several studies.[54] Of interest, the same has been reported for families with ADTKD-*UMOD*.[64] Therefore, we assume that the purely descriptive histologic findings of glomerular segmental scleroses are secondary in nature, as would be the moderate extent of proteinuria, which can develop. More important, even with the knowledge of the molecular diagnoses, we could not clearly recognize unambiguous histologic or ultrastructural features of these diseases on reanalysis of the biopsies (Figures 2 and 4). Thus, any workup for hereditary kidney diseases should not restrict the virtual panel of genes to be analyzed too early.

Therefore, in our view, a contemporary workflow for genetic analysis of families suspected for ADTKD should ideally use an exome-wide platform from the beginning. Clinical and (if available) histologic information should be recorded to choose the appropriate panel of known disease genes, which can successively be screened for variants. Considering the relatively high frequency of collagen IV–associated diseases in such cohorts and the relative ease of analysis, we would investigate the respective *COL4* genes early on after exclusion of the known ADTKD candidate genes (Figure 8). Should these efforts not yield a diagnostic mutation, *MUC1* VNTR analysis should be performed and the pedigree checked for compatibility with mitochondrial diseases. Further options will then be analysis of the *nephrome* and the exome, as well as searching for an atypical *MUC1* mutation. However, many of these options will probably need to be performed by a specialized and/or academically interested laboratory. At this point, it is important to stress that the full spectrum of analyses cannot be expected on a routine clinical basis. The blurred transition from clinical diagnostics to research interest and broad genetic analysis also has ethical implications and should be recognized in the patient consent.[65]

DISCLOSURE

All the authors declared no competing interests.

DATA STATEMENT

For reasons of data protection, we prefer not to deposit exome sequencing of probands in a public repository. However, interested scientists are welcome to contact us and request the data.

ACKNOWLEDGMENTS

This work was performed in fulfillment of the requirements for obtaining the degree Doctor of Medicine (Dr. med.) by FJW, who was supported by the Interdisciplinary Center for Clinical Research (IZKF) at the University Hospital of the University of Erlangen-Nürnberg

(MD-Thesis Scholarship Program). Part of this research was made possible through access to the data and findings generated by the 100,000 Genomes Project. Additional details for the Genomics England 100,000 Genomes Project are shown in the Supplementary Methods. The graphical Figure 8 was created by using Servier Medical Art templates, which are licensed under a Creative Commons Attribution 3.0 Unported Licence (https://smart.servier.com).

The studies were funded by the Deutsche Forschungsgemeinschaft (German Research Foundation)–Project Number 387509280–SFB 1350, TP C4, A5, C6, and C2, as well as partially by the Else Kröner-Fresenius-Stiftung and the Eva Luise und Horst Köhler Stiftung–Project Number 2019_KollegSE.04: "Research Center on Rare Kidney Diseases." Additional support by the Interdisciplinary Center for Clinical Research Erlangen to TJ-S (project number J70). BP is supported by the Deutsche Forschungsgemeinschaft through grant PO2366/2–1.

SUPPLEMENTARY MATERIAL

Supplementary File (Word)

Figure S1. Structural impacts of missense mutations detected by *nephrome* analysis. Structural impact of missense mutations in proteins encoding for selected genes listed in Table 4 were assessed by α-fold structure predictions and docking. (**A**) Exchange of Gly1451 against a valine residue close to the noncollagenous C-terminal domain (C-NC) of *COL4A5* and of the positively charged Arg1677 against the polar glutamine residue in the C-NC might disturb proper trimerization and subsequent hexamerization, which are key to the collagen networking (based on the α-fold model AF-P29400-F1-model_v2.pdb 1430-1680 and the pdb entry code 5naz). (**B**) Nonconservative exchange of Gly624, which is part of the repetitive G-X-Y motif (in green) in the long collagenous region of *COL4A5* against a negatively charged aspartate residue, most likely affects formation of the coiled triple helix (inset). As the G-X-Y- motif is already naturally interrupted at position G626 (red box),[S1] G624D would affect the triple helix conformation significantly. (**C**) Exchange of the negatively charged Asp255 against the polar asparagine residue in the diaphanous inhibitory domain (DID) of inverted-formin-2 proteins *INF2* and of Gln71 against a proline just in front of the G-domain of *INF2* (AF-Q2781-F1-model-v2.pdb) would interfere with ionic interactions (e.g., between Asp255 and Arg214; inset). This missense mutation might affect the super helical coil of the armadillo repeat of the DID domain (orange) with likely consequences on Rho-GTPase binding and *INF2* dimerization, which play a role in nucleation and elongation of actin filaments.

Figure S2. Protein-protein interaction network between autosomal dominant tubulointerstitial kidney disease (ADTKD) genes and novel candidates. Molecular network generated by the STRING protein interaction database using the 5 known ADTKD genes and 27 novel candidate genes as input. Line color indicates type of interaction evidence, as shown in the figure.

Table S1. Published *MUC1* frameshift mutations.

Table S2. Heterozygous *nephrome* variants in relation to clinical characteristics.

Table S3. Validation of the diagnostic copy number variants (CNVs) and splice site variant identified by *nephrome* analysis.

Table S4. Single-molecule, real-time (SMRT) sequencing of the *MUC1* VNTR.

Table S5. Genetic variants identified in exome analysis.

Table S6. Estimated glomerular filtration rate (eGFR) association and expression quantitative trait loci variants (eQTLs) for regions around the 5 known and 27 putative novel autosomal dominant tubulointerstitial kidney disease (ADTKD) genes.

Table S7. Biobank data of putative novel renal candidate genes.

Supplementary Methods.

Supplementary Clinical Notes. Clinical description of autosomal dominant tubulointerstitial kidney disease (ADTKD)–not otherwise specified (NOS) families.

Figure S3. Pedigree of family A-1.

Figure S4. Pedigree of family A-2.

Figure S5. Pedigree of family A-7.

Figure S6. Pedigree of family A-8.

Figure S7. Pedigree of family A-17.

Figure S8. Pedigree of family A-26.

Figure S9. Pedigree of family A-31.

Figure S10. Kidney biopsy of affected individual in family A-31.

Figure S11. Pedigree of family A-42.

Figure S12. Pedigree of family A-48.

Figure S13. Pedigree of family A-49.

Figure S14. Pedigree of family A-51.

Figure S15. Pedigree of family A-52.

Figure S16. Pedigree of family A-53.

Figure S17. Kidney biopsy of affected individual in family A-53.

Figure S18. Pedigree of family A-54.

Figure S19. Townes-Brocks syndrome, causative for hypoplastic right thumb.

Figure S20. Pedigree of family A-56.

Figure S21. Kidney biopsy of affected individual in family A-56.

Figure S22. Pedigree of family A-57.

Supplementary References.

REFERENCES

1. Vivante A, Hildebrandt F. Exploring the genetic basis of early-onset chronic kidney disease. *Nat Rev Nephrol*. 2016;12:133–146.
2. Devuyst O, Knoers NV, Remuzzi G, et al. Rare inherited kidney diseases: challenges, opportunities, and perspectives. *Lancet*. 2014;383:1844–1859.
3. Rasouly HM, Groopman EE, Heyman-Kantor R, et al. The burden of candidate pathogenic variants for kidney and genitourinary disorders emerging from exome sequencing. *Ann Intern Med*. 2019;170:11–21.
4. Groopman EE, Marasa M, Cameron-Christie S, et al. Diagnostic utility of exome sequencing for kidney disease. *N Engl J Med*. 2019;380:142–151.
5. Hays T, Groopman EE, Gharavi AG. Genetic testing for kidney disease of unknown etiology. *Kidney Int*. 2020;98:590–600.
6. Cocchi E, Nestor JG, Gharavi AG. Clinical genetic screening in adult patients with kidney disease. *Clin J Am Soc Nephrol*. 2020;15:1497–1510.
7. Eckardt KU, Alper SL, Antignac C, et al. Autosomal dominant tubulointerstitial kidney disease: diagnosis, classification, and management-a KDIGO consensus report. *Kidney Int*. 2015;88:676–683.
8. Devuyst O, Olinger E, Weber S, et al. Autosomal dominant tubulointerstitial kidney disease. *Nat Rev Dis Primers*. 2019;5:60.
9. Kidd K, Vylet'al P, Schaeffer C, et al. Genetic and clinical predictors of age of ESKD in individuals with autosomal dominant tubulointerstitial kidney disease due to UMOD mutations. *Kidney Int Rep*. 2020;5:1472–1485.
10. Bleyer AJ, Kmoch S, Antignac C, et al. Variable clinical presentation of an MUC1 mutation causing medullary cystic kidney disease type 1. *Clin J Am Soc Nephrol*. 2014;9:527–535.
11. Hart TC, Gorry MC, Hart PS, et al. Mutations of the *UMOD* gene are responsible for medullary cystic kidney disease 2 and familial juvenile hyperuricaemic nephropathy. *J Med Genet*. 2002;39:882–892.
12. Kirby A, Gnirke A, Jaffe DB, et al. Mutations causing medullary cystic kidney disease type 1 lie in a large VNTR in MUC1 missed by massively parallel sequencing. *Nat Genet*. 2013;45:299–303.
13. Lindner TH, Njolstad PR, Horikawa Y, et al. A novel syndrome of diabetes mellitus, renal dysfunction and genital malformation associated with a partial deletion of the pseudo-POU domain of hepatocyte nuclear factor-1beta. *Hum Mol Genet*. 1999;8:2001–2008.
14. Zivna M, Hulkova H, Matignon M, et al. Dominant renin gene mutations associated with early-onset hyperuricemia, anemia, and chronic kidney failure. *Am J Hum Genet*. 2009;85:204–213.
15. Bolar NA, Golzio C, Zivna M, et al. Heterozygous loss-of-function SEC61A1 mutations cause autosomal-dominant tubulo-interstitial and glomerulocystic kidney disease with anemia. *Am J Hum Genet*. 2016;99:174–187.

16. Knaup KX, Hackenbeck T, Popp B, et al. Biallelic expression of mucin-1 in autosomal dominant tubulointerstitial kidney disease: implications for nongenetic disease recognition. *J Am Soc Nephrol*. 2018;29:2298–2309.
17. Ayasreh N, Bullich G, Miquel R, et al. Autosomal dominant tubulointerstitial kidney disease: clinical presentation of patients with ADTKD-UMOD and ADTKD-MUC1. *Am J Kidney Dis*. 2018;72:411–418.
18. Cormican S, Connaughton DM, Kennedy C, et al. Autosomal dominant tubulointerstitial kidney disease (ADTKD) in Ireland. *Ren Fail*. 2019;41:832–841.
19. Olinger E, Hofmann P, Kidd K, et al. Clinical and genetic spectra of autosomal dominant tubulointerstitial kidney disease due to mutations in UMOD and MUC1. *Kidney Int*. 2020;98:717–731.
20. Gong K, Xia M, Wang Y, et al. Autosomal dominant tubulointerstitial kidney disease genotype and phenotype correlation in a Chinese cohort. *Sci Rep*. 2021;11:3615.
21. Ekici AB, Hackenbeck T, Moriniere V, et al. Renal fibrosis is the common feature of autosomal dominant tubulointerstitial kidney diseases caused by mutations in mucin 1 or uromodulin. *Kidney Int*. 2014;86:589–599.
22. Zivna M, Kidd K, Pristoupilova A, et al. Noninvasive immunohistochemical diagnosis and novel MUC1 mutations causing autosomal dominant tubulointerstitial kidney disease. *J Am Soc Nephrol*. 2018;29:2418–2431.
23. Yamamoto S, Kaimori JY, Yoshimura T, et al. Analysis of an ADTKD family with a novel frameshift mutation in MUC1 reveals characteristic features of mutant MUC1 protein. *Nephrol Dial Transplant*. 2017;32:2010–2017.
24. Moriniere V, Hollebecque S, S. L, et al. Mutations in a large VNTR of MUC1 are frequent in autosomal dominant medullary cystic kidney disease (MCKD). *J Am Soc Nephrol Abstract Suppl*. 2013;24:68A.
25. Dvela-Levitt M, Kost-Alimova M, Emani M, et al. Small molecule targets TMED9 and promotes lysosomal degradation to reverse proteinopathy. *Cell*. 2019;178:521–535.e523.
26. Connor TM, Hoer S, Mallett A, et al. Mutations in mitochondrial DNA causing tubulointerstitial kidney disease. *PLoS Genet*. 2017;13:e1006620.
27. Wenzel A, Altmueller J, Ekici AB, et al. Single molecule real time sequencing in ADTKD-MUC1 allows complete assembly of the VNTR and exact positioning of causative mutations. *Sci Rep*. 2018;8:4170.
28. Li H, Durbin R. Fast and accurate short read alignment with Burrows-Wheeler transform. *Bioinformatics*. 2009;25:1754–1760.
29. Wang K, Li M, Hakonarson H. ANNOVAR: functional annotation of genetic variants from high-throughput sequencing data. *Nucleic Acids Res*. 2010;38:e164.
30. Hauer NN, Popp B, Schoeller E, et al. Clinical relevance of systematic phenotyping and exome sequencing in patients with short stature. *Genet Med*. 2018;20:630–638.
31. Kircher M, Witten DM, Jain P, et al. A general framework for estimating the relative pathogenicity of human genetic variants. *Nat Genet*. 2014;46:310–315.
32. Pollard KS, Hubisz MJ, Rosenbloom KR, et al. Detection of nonneutral substitution rates on mammalian phylogenies. *Genome Res*. 2010;20:110–121.
33. Davydov EV, Goode DL, Sirota M, et al. Identifying a high fraction of the human genome to be under selective constraint using GERP++. *PLoS Comput Biol*. 2010;6:e1001025.
34. Cartegni L, Wang J, Zhu Z, et al. ESEfinder: a web resource to identify exonic splicing enhancers. *Nucleic Acids Res*. 2003;31:3568–3571.
35. den Dunnen JT, Dalgleish R, Maglott DR, et al. HGVS recommendations for the description of sequence variants: 2016 update. *Hum Mutat*. 2016;37:564–569.
36. Richards S, Aziz N, Bale S, et al. Standards and guidelines for the interpretation of sequence variants: a joint consensus recommendation of the American College of Medical Genetics and Genomics and the Association for Molecular Pathology. *Genet Med*. 2015;17:405–424.
37. Visscher PM, Wray NR, Zhang Q, et al. 10 Years of GWAS discovery: biology, function, and translation. *Am J Hum Genet*. 2017;101:5–22.
38. Stanzick KJ, Li Y, Schlosser P, et al. Discovery and prioritization of variants and genes for kidney function in >1.2 million individuals. *Nat Commun*. 2021;12:4350.
39. Gillies CE, Putler R, Menon R, et al. An eQTL landscape of kidney tissue in human nephrotic syndrome. *Am J Hum Genet*. 2018;103:232–244.
40. Sheng X, Guan Y, Ma Z, et al. Mapping the genetic architecture of human traits to cell types in the kidney identifies mechanisms of disease and potential treatments. *Nat Genet*. 2021;53:1322–1333.
41. GTEx Consortium, Laboratory, Data Analysis, & Coordinating Center (LDACC)—Analysis Working Group, Statistical Methods groups—Analysis Working Group, et al. Genetic effects on gene expression across human tissues. *Nature*. 2017;550:204–213.
42. Szklarczyk D, Gable AL, Lyon D, et al. STRING v11: protein-protein association networks with increased coverage, supporting functional discovery in genome-wide experimental datasets. *Nucleic Acids Res*. 2019;47:D607–D613.
43. Williams SE, Reed AA, Galvanovskis J, et al. Uromodulin mutations causing familial juvenile hyperuricaemic nephropathy lead to protein maturation defects and retention in the endoplasmic reticulum. *Hum Mol Genet*. 2009;18:2963–2974.
44. Sanna-Cherchi S, Khan K, Westland R, et al. Exome-wide association study identifies GREB1L mutations in congenital kidney malformations. *Am J Hum Genet*. 2017;101:1034.
45. Dahan K, Devuyst O, Smaers M, et al. A cluster of mutations in the *UMOD* gene causes familial juvenile hyperuricemic nephropathy with abnormal expression of uromodulin. *J Am Soc Nephrol*. 2003;14:2883–2893.
46. Bokhove M, Nishimura K, Brunati M, et al. A structured interdomain linker directs self-polymerization of human uromodulin. *Proc Natl Acad Sci U S A*. 2016;113:1552–1557.
47. So WY, Ng MC, Horikawa Y, et al. Genetic variants of hepatocyte nuclear factor-1beta in Chinese young-onset diabetic patients with nephropathy. *J Diabetes Complications*. 2003;17:369–373.
48. Olinger E, Schaeffer C, Kidd K, et al. An intermediate effect size variant in *UMOD* confers risk for chronic kidney disease. Preprint. Posted online October 2, 2021. *medRxiv*. https://doi.org/10.1101/2021.09.27.21263789
49. Barua M, Stellacci E, Stella L, et al. Mutations in PAX2 associate with adult-onset FSGS. *J Am Soc Nephrol*. 2014;25:1942–1953.
50. Amiel J, Audollent S, Joly D, et al. PAX2 mutations in renal-coloboma syndrome: mutational hotspot and germline mosaicism. *Eur J Hum Genet*. 2000;8:820–826.
51. Reardon W, Casserly LF, Birkenhager R, et al. Kidney failure in Townes-Brocks syndrome: an under recognized phenomenon? *Am J Med Genet A*. 2007;143A:2588–2591.
52. Posey JE, Harel T, Liu P, et al. Resolution of disease phenotypes resulting from multilocus genomic variation. *N Engl J Med*. 2017;376:21–31.
53. Lata S, Marasa M, Li Y, et al. Whole-exome sequencing in adults with chronic kidney disease: a pilot study. *Ann Intern Med*. 2018;168:100–109.
54. Papazachariou L, Papagregoriou G, Hadjipanagi D, et al. Frequent COL4 mutations in familial microhematuria accompanied by later-onset Alport nephropathy due to focal segmental glomerulosclerosis. *Clin Genet*. 2017;92:517–527.
55. Pierides A, Voskarides K, Kkolou M, et al. X-linked, COL4A5 hypomorphic Alport mutations such as G624D and P628L may only exhibit thin basement membrane nephropathy with microhematuria and late onset kidney failure. *Hippokratia*. 2013;17:207–213.
56. Zurowska AM, Bielska O, Daca-Roszak P, et al. Mild X-linked Alport syndrome due to the COL4A5 G624D variant originating in the Middle Ages is predominant in Central/East Europe and causes kidney failure in midlife. *Kidney Int*. 2021;99:1451–1458.
57. Ninomiya Y, Kagawa M, Iyama K, et al. Differential expression of two basement membrane collagen genes, COL4A6 and COL4A5, demonstrated by immunofluorescence staining using peptide-specific monoclonal antibodies. *J Cell Biol*. 1995;130:1219–1229.
58. Abreu-Velez AM, Howard MS. Collagen IV in normal skin and in pathological processes. *N Am J Med Sci*. 2012;4:1–8.
59. Gubler MC. Inherited diseases of the glomerular basement membrane. *Nat Clin Pract Nephrol*. 2008;4:24–37.
60. Groopman EE, Povysil G, Goldstein DB, et al. Rare genetic causes of complex kidney and urological diseases. *Nat Rev Nephrol*. 2020;16:641–656.
61. Freedman BI, Volkova NV, Satko SG, et al. Population-based screening for family history of end-stage renal disease among incident dialysis patients. *Am J Nephrol*. 2005;25:529–535.
62. Skrunes R, Svarstad E, Reisaeter AV, et al. Familial clustering of ESRD in the Norwegian population. *Clin J Am Soc Nephrol*. 2014;9:1692–1700.
63. Popp B, Ekici AB, Knaup KX, et al. Prevalence of hereditary tubulointerstitial kidney diseases in the German Chronic Kidney Disease study. Preprint. Posted online September 30, 2021. *medRxiv*. https://doi.org/10.1101/2021.09.29.21264100
64. Chun J, Wang M, Wilkins MS, et al. Autosomal dominant tubulointerstitial kidney disease-uromodulin misclassified as focal segmental glomerulosclerosis or hereditary glomerular disease. *Kidney Int Rep*. 2020;5:519–529.
65. Mallett AJ, Knoers N, Sayer J, et al. Clinical versus research genomics in kidney disease. *Nat Rev Nephrol*. 2021;17:570–571.